# REPORT DOCUMENTATION PAGE

*Form Approved*
*OMB No. 074-0188*



| 1. AGENCY USE ONLY (Leave blank) | 2. REPORT DATE | 3. REPORT TYPE AND DATES COVERED |
|---|---|---|
| | 3/2/2007 | Final Report 5/1/2003 to 7/31/2006 |

**4. TITLE AND SUBTITLE**
A 10,000-Pen Nanoplotter with Integrated Ink Delivery Systems

**5. FUNDING NUMBERS**
DAAD19-03-1-0065

**6. AUTHOR(S)**
Chad A. Mirkin

**7. PERFORMING ORGANIZATION NAME(S) AND ADDRESS(ES)**

Northwestern University
Department of Chemistry
2145 Sheridan Road
Evanston, IL 60208

**8. PERFORMING ORGANIZATION REPORT NUMBER**

**9. SPONSORING / MONITORING AGENCY NAME(S) AND ADDRESS(ES)**

U.S. Army Research Office
P.O. Box 12211
Research Triangel Park, NC 27709-2211

**10. SPONSORING / MONITORING AGENCY REPORT NUMBER**

45139.1-PH-DRP

**11. SUPPLEMENTARY NOTES**

**12a. DISTRIBUTION / AVAILABILITY STATEMENT**

Approved for public release; Distribution Unlimited

**12b. DISTRIBUTION CODE**

**13. ABSTRACT** ***(Maximum 200 Words)***

This report summarizes major scientific and technological accomplishments during the three years of this grant. It includes an extensive list of articles published in peer reviewed journals and participation in scientific meetings, workshops, and lectures. Finally, patent disclosures, transitions, and awards earned by the participating investigators are listed. Over the three-year project period significant progress has been made in both areas. The **Liu** group took the lead in developing new DPN hardware and developed many advanced tools for SPL including 1-D and 2-D passive arrays, a 1-D active probe array, polydimethylsiloxane (PDMS) passive probes, a multifunctional active probe array and a microfluidic inking chip, and the development of electrostatic actuation probes. The advanced scanning probes and probe arrays that were developed under this program expanded the capabilities of scanning probe nanolithography (SPL) and have advanced SPL technology for commercial applications. **Mirkin** focused on the development of new DPN applications in particular the development of protocols for the fabrication of electronically active nanostructures, for biodetection, and multiple-pen DPN.

While the majority of important milestones was reached, as well as exceeded future challenges remain. Currently the main challenge in the field of Dip-Pen Nanolithography is to develop protocols for the fabrication of multi-component nanoarrays composed of different biological and chemical molecules.

**14. SUBJECT TERMS**
Dip-Pen Nanolithography, AFM, protein nanoarrays, DPN hardware, microfluidic inking chip

**15. NUMBER OF PAGES**

**16. PRICE CODE**

| 17. SECURITY CLASSIFICATION OF REPORT | 18. SECURITY CLASSIFICATION OF THIS PAGE | 19. SECURITY CLASSIFICATION OF ABSTRACT | 20. LIMITATION OF ABSTRACT |
|---|---|---|---|
| | | | UU |

## TABLE OF CONTENT

## SUMMARY

This report summarizes major scientific and technological accomplishments during the three years of this grant. It includes an extensive list of articles published in peer reviewed journals and participation in scientific meetings, workshops, and lectures. Finally, patent disclosures, transitions, and awards earned by the participating investigators are listed. The three years of this project were exceptionally productive as can be deduced from the highlights of the scientific and technological breakthroughs in the following paragraph. The focus of our effort was in two major areas:

A – Development of new Dip-Pen Nanolithography (DPN) hardware
B – Development of DPN chemistry and applications

Over the three-year project period significant progress has been made in both areas. The **Liu** group took the lead in developing new DPN hardware and developed many advanced tools for SPL including 1-D and 2-D passive arrays, a 1-D active probe array, polydimethylsiloxane (PDMS) passive probes, a multifunctional active probe array and a microfluid inking chip, and the development of electrostatic actuation probes. The advanced scanning probes and probe arrays that were developed under this program expanded the capabilities of scanning probe nanolithography (SPL) and have advanced SPL technology for commercial applications. **Mirkin** focused on the development of new DPN applications in particular the development of protocols for the fabrication of electronically active nanostructures, for biodetection, and multiple-pen DPN.

While the majority of important milestones was reached, as well as exceeded future challenges remain. Currently the main challenge in the field of Dip-Pen Nanolithography is to develop protocols for the fabrication of multicomponent nanoarrays composed of different biological and chemical molecules

With regard to other accomplishments, many postdoctoral associates and graduate students were trained in areas of vital importance to the mission of the DOD, with potential payoff for the agency in the near future, and the long-term deployment of many DPN-based applications. The highlights of our accomplishments are featured in the following report.

## PUBLICATIONS

### A. Manuscripts Submitted

1. Dellinger, T.; Li, S.; Wang, Q.; Liu, C. "Pneumatic Actuated PDMS Devices for Surface Patterning ," *Langmuir*, **2006**, submitted.
2. Jang, J.-W., Maspoch, D.; Fujigaya, T.; Mirkin, C.A. "A Molecular Eraser for Dip-Pen Nanolithography," *Small* **2006**, submitted.

### B. Publications in Peer-Reviewed Journals

1. Bullen, D.; Chung, S.W.; Wang, X.; Zou, J.; Mirkin, C. A.; Liu, C. "Parallel Dip-Pen Nanolithography with arrays of individually addressable cantilevers," *Applied Physics Letters* **2004**, 84 (5), 789-791.
2. Bullen, D., Wang, X., Zou, J., Chung, S.-W., Mirkin, C.A., Liu, C. "Design, Fabrication, and Characterization of Thermally Actuated Probe Arrays for Dip Pen Nanolithography," *IEEE/ASME Journal of Microelectromechanical Systems*, **2004**, *13(4)*, 594-602.
3. Chung, S.–W.; Ginger, D.S.; Morales, M.; Zhang, Z.; Chandrasekhar, V.; Ratner, M.A.; Mirkin, C.A. "Top-Down Meets Bottom-Up: Dip-Pen Nanolithography and DNA-Directed Assembly of Nanoscale Electrical Circuits" *Small* **2005,** *1*, 64-69.
4. Fu, L.; Liu, X.; Zhang, Y.; Dravid, V.P.; Mirkin, C.A.; "Nanopatterning of "Hard" Magnetic Nanostructures via Dip-Pen Nanolithography and a Sol-Based Ink," *Nano Lett.* **2003**, *3*, 757-760.
5. Ginger, D.S.; Zhang, H.; Mirkin, C.A. "The Evolution of Dip-Pen Nanolithography," *Angew. Chem. Int. Ed.* **2004**, *43*, 30 – 45.
6. Huang, L.; Chang, Y.-H.; Kakkassery, J. J.; Mirkin, C.A. "Dip-Pen Nanolithography of High Melting-Temperature Molecules," *J. Phys. Chem. B.*, **2006**,*110*, 20756-20758.
7. Huo, F.; Lytton-Jean, A.K.R.; Mirkin, C.A. "Asymmetric Functionalization of Nanoparticles Based on Thermally Addressable DNA Interconnects," *Adv. Mater.,* **2006**, *18*, 2304-2306.
8. Jin, R.; Cao, Y.C., Thaxton, C.S.; Mirkin, C.A. "Glass-Bead-Based Parallel Detection of DNA Using Composite Raman Labels," *Small*, **2006**, *2*, 375-380.
9. Lee, J.–S.; Stoeva, S.I.; Mirkin, C.A. "DNA-Induced Size-Selective Separation of Mixtures of Gold Nanoparticles," *J. Am. Chem. Soc.*, **2006**, *128*, 8899-8903
10. Lee, K-B.; Lim, J-H.; Mirkin, C.A. "Protein Nanostructures Formed Via Direct-Write Dip-Pen Nanolithography," *J. Am. Chem. Soc.* **2003**, *125*, 5588-5589.
11. Lee, K-B.; Smith, J.C.; Wang, Q.; Finn, M.G.; Johnson, J.E.; Mrksich, M.; Mirkin, C.A.; "Nanopatterning the Chemospecific Immobilization of Cowpea Mosaic Virus Capsid," *Nano Lett.* **2003**, *3*, 883-886.
12. Lee, K.–B.; Kim, E.-Y.; Mirkin, C.A.; Wolinsky, S. M. "The Use of Nanoarrays for Highly Sensitive and Selective Detection of Human Immunodeficiency Virus Type 1 in Plasma" *Nano Lett.* **2004,** *4*, 1869 - 1872.
13. Lee, K–B.; Park, S.; Mirkin, C.A. "Multicomponent Magnetic Nanorods for Biomolecular Separations" *Angew. Chem. Int. Ed.* **2004**, *43*, 3048-3050.
14. Li, S.; Shaikh, K.A.; Szegedi, S.; Goluch, E.; Liu, C. "A Micromachined Inking Chip for Scanning Probe Nanolithography Using Local Vapor Inking Method", Applied Physics Letter, **2006,** in press.

15. Lim, J-H.; Ginger, D.S.; Lee, K-B.; Heo, J.; Nam, J-M.; Mirkin, C.A. "Direct-Write Dip-Pen Nanolithography of Proteins on Modified Silicon Oxide Surfaces," *Angew. Chem.* **2003**, *20,* 2411-2414.
16. Liu, X.; Guo, S.; Mirkin, C.A. "Surface and Site-Specific Ring-Opening Metathesis Polymerization Initiated by Dip-Pen Nanolithography," *Angew. Chem. Int. Ed.* **2003**, *115*, 4933-4937.
17. Lytton-Jean, A.; Mirkin, C.A. "A Thermodynamic Investigation into the Binding Properties of DNA Functionalized Gold Nanoparticle Probes and Molecular Fluorophore Probes" *J. Am. Chem. Soc.* **2005**, in press.
18. Park, S.; Chung, S.-W.; Mirkin, C.A. "Hybrid Organic-Inorganic, Rod-Shaped Nanoresistors and Diodes" *J. Am. Chem. Soc*. **2004**, *126*, 11772-11773.
19. Park, S.-J.; Lazarides, A.A.; Storhoff, J. J.; Pesce, L.; Mirkin, C.A. "The Structural Characterization of Oligonucleotide-Modified Gold Nanoparticle Networks Formed by DNA Hybridization" *J. Phys. Chem. B.* **2004**, *108*, 12375-12380.
20. Qin, L.; Park, S.; Mirkin, C.A. "On-Wire Lithography (OWL)" *Science* **2005**, *309*, 113-115.
21. Qin, L.; Jang, J.W.; Huang, L.; Mirkin, C.A. "Sub-5 nm Gaps by On-Wire Lithography: Correlating Gap Size with Electrical Transport," *Small*, **2007**, *3*, 86-90.
22. Rosi, N.L.; Mirkin, C.A. "Nanostructures in Biodiagnostics" *Chem Rev.* **2005**, *105*, 1547-1562.
23. Rosi, N.; Thaxton, C.S.; Mirkin, C.A. "Control of Nanoparticle Assembly Using DNA-Modified Diatom Templates" *Angew Chem Int. Ed.* **2004,** *43*, 5500-5503.
24. Ryu, K., Wang, X., Shaikh, K., Liu, C. "A Method for Precision Patterning of Silicone Eastover and Its Applications," *IEEE/ASME Journal of Microelectromechanical Systems*, **2004**, *13(4)*, 568-575.
25. Rozhok, S.; Piner, R.; Mirkin, C.A. "Dip-Pen Nanolithography: What Controls Ink Transport?" *J. Phys. Chem. B* **2003**, *107*, 751-757.
26. Rozhok, S.; Sun, P.; Piner, R.; Lieberman, M.; Mirkin, C.A. "AFM Study of Water Meniscus Formation between an AFM Tip and NaCl Substrate," *J. Phys. Chem. B,* **2004**, *108*, 7814-7819.
27. Rozhok, S.; Shen, C. K-F.; Littler, P-L. H.; Fan, Z.; Liu, C.; Mirkin, C.A.; Holtz, R.C. "Methods for Fabrication Microarrays of Motile Bacteria" *Small* **2005,** *4*, 445-451.
28. Ryu, K., Wang, X., Shaikh, K., Bullen, D., Goluch, E., Zou, J., Liu, C., Mirkin, C.A. "Integrated Microfluidic Inking Chip for Scanning Probe Nanolithography," *Applied Physics Letters*, **2004**, *85(1),* 136-138.
29. Salaita, K.; Amarnath, A.; Higgins, T.B.; Mirkin, C.A. "Spontaneous Phase Separation of Patterned Binary Alkanethiol Mixtures," *J. Am. Chem. Soc.* **2005**, *127,* 11283-11287.
30. Salaita, K., Lee, S.-W., Wang, X., Huang, L., Dellinger, T., Liu, C., Mirkin, C.A. "Sub-100 nm, Centimeter-Scale, Parallel Dip-Pen Nanolithography," *Small*, **2005**, *10*, 940-945.
31. Salaita, K.S.; Lee, S.W.; Ginger D.S.; Mirkin. C.A. "DPN-Generated Nanostructures as Positive Resists for Preparing Lithographic Masters or Hole Arrays," *Nano Letters*, **2006**, *6*, 2493-2498.
32. Salaita, K.S.; Mirkin, C.A. "Applications of Dip-Pen Nanolithography," *Nature Nanotech*. **2006**, in press.
33. Salaita, K.S.; Wang, Y.; Fragala, J.; Liu, C.; Mirkin, C.A. "Massively Parallel Dip-Pen Nanolithography With 55,000-Pen Two-Dimensional," *Angew. Chem. Int Ed.*, **2006**, *45*, 7220-7223.

34. Thaxton, C.S.; Rosi, N.L.; Mirkin, C.A. "Optically and Chemically Encoded Nanoparticle Materials in Biomolecule Detection," *MRS Bulletin*, **2005**, *30*, 376-380.
35. Vega, R.A.; Maspoch, D.; Salaita, K. Mirkin, C.A. "Nanoarrays of Single Virus Particles," *Angew. Chem.,* **2005**, *44*, 6013-6015.
36. Vega, R.A.; Maspoch, D.; Shen, C. K.-F.; Kakkassery, J.J.; Chen, B.J.; Fujigaya, T.; Lamb, R.A.; Mirkin, C.A. "Functional Antibody Arrays through Metal Ion Affinity Templates," *ChemBioChem,* **2006**, *7*, 1653-1657.
37. Wang, X.; Bullen, D.; Zou, J.; Zhang, H.; Liu, C.; Mirkin, C.A. "Scanning Probe Contact Printing," *Langmuir* 2003, *19*, 8951-8955.
38. Wang, X, Bullen, D., Zou, J., Liu, C., Mirkin, C.A. **"**A Thermally Actuated Probe Array For Parallel Dip Pen Nanolithography," *Journal of Vacuum Science and Technology B*, **2004**, *22(6),* 2563-2567.
39. Wang, X.; Liu, C. "Multifunctional Probe Array for Nano Patterning and Imaging," *Nano Letters*, **2005**, *5*, 1867-1872.
40. Wang, X., Vincent, L., Bullen, D., Zou, J., Liu, C. "Scanning Probe Lithography Tips with Spring-on-Tip Designs: Analysis, Fabrication, and Testing", *Applied Physics Letters*, **2005**, in press.
41. Wang, Y.; Maspoch, D.; Zou, S.; Schatz, G.C.; Smalley, R.E.; Mirkin, C.A. "Controlling the shape, orientation and linkage of carbon nanotube features with nano affinity templates," *Proc. Natl. Acad. Sci,* **2006**, *103,* 2026-2031.
42. Xu, X.-Y.; Rosi, N.L.; Wang, Y.; Huo, F.; Mirkin, C.A. "Asymmetric Functionalization of Gold Nanoparticles with Oligonucleotides," *J. Am. Chem. Soc.*, **2006**, *128,* 9286-9287.
43. Zhang, H.; Chung, S.-W.; Mirkin, C.A. "Fabrication of sub-50 nm Solid-State Nanostructures Based on Dip-Pen Nanolithography," *Nano Lett.* **2003**, *1*, 43-45.
44. Zhang, H.; Lee, K-B.; Li, Z.; Mirkin, C.A. "Biofunctionalized Nanoarrays of Inorganic Structures Prepared by Dip-Pen Nanolithography," *Nanotechnology* **2003**, *14*, 1113-1117.
45. Zhang, Y.; Salaita, K.; Lim, J.H.; Lee, K.-B.; Mirkin, C.A. "A Massively Parallel Electrochemical Approach to the Miniaturization of Organic Micro and Nanostructures on Surfaces," *Langmuir,* **2004**, *20*, 962-968.
46. Zhou, S.; Maspoch, D.; Wang, Y.; Mirkin, C.A.; Schatz, G. "Rings of Single-Walled Carbon Nanotubes: Molecular-Template Directed Assembly and Monte-Carlo Modeling," *Nano Letters*, **2006**, in press.
47. Zou, J.; Bullen, D.; Wang, X.; Liu, C.; Mirkin, C.A., "Conductivity-based Contact Sensing for Probe Arrays in Dip-Pen Nanolithography," *Appl. Phys. Lett.* **2003**, *83*, 581-583.
48. Zou, J.; Wang, X.; Bullen, D.; Ryu, K.; Liu, C.; Mirkin, C.A "A Mould-and-Transfer Technology for Fabricating Scanning Probe Microscopy (SPM) Probes," *Journal of Micromechanics and Microengineering* **2004**, *14*, 204-211.

## C. Conference Proceedings

1. Wang, X.; Ryu, K.; Bullen, D.; Zou, J.; Mirkin, C.A.; Liu, C. "Scanning Probe with Elastomeric (PDMS) Tip for Scanning Probe Microcontact Printing (SP-μCP)," Proceedings of the 12th International Conference on Solid-State Sensors, Actuators and Microsystems, pp. 1003-1006, Boston, MA, 8-12 June 2003.
1. Li, S.; Liu, C. "MEMS Arrayed Scanning Probes for Soft Nanolithography," Electrochemical Society Transactions, Volume 3, MEMS/NEMS 7, October 29-November 3, 2006, Cancun, Mexico.

**D. Presentations at Meetings**

1. BNI & IFBT 2006, "Arrayed Multifunctional Scanning Probes for Soft Nanolithography and Direct Writing Bioarray," (Li, S.; Wang, Q.; Padua, G.W.; Liu, C., 2006)**.**
2. DARPA, San Francisco, CA, "Tip-Based Nano Fabrication," (Mirkin, C.A.;2006).
3. Warren Lecture, Vanderbilt University, Nashville, TN, "The Evolution of Massively Parallel Dip-Pen Nanolithography," (Mirkin, C.A.; 2006).
4. Pauling Symposium, Western Washington University, Bellingham, WA, "The Evolution of Massively Parallel Dip-Pen," (Mirkin, C.A.; 2006).
5. MESA/Institute for Nano, September 27, 2006, University of Twente, Enschede, Netherlands, "Unconventional Approaches to Nanofabrication," (Mirkin, C.A.; 2006).
6. TNT 2006 Conference, Grenoble, France; "Novel Approaches to Nanostructure Assembly and Nanofabrication," (Mirkin, C.A.; 2006).
7. ICN+T 2006: International Conference on Nanoscience and Technology, Basel, Switzerland; "Massively Parallel Dip Pen Nanolithography," (Mirkin, C.A.; 2006).
8. BASF Meeting, Ludwigshafen, Germany; "Massively Parallel Dip-Pen Nanolithography" (Mirkin, C.A.; 2006).
9. AACC Annual Meeting, Chicago, IL; "Nanotechnological Tools That Will Impact Molecular Diagnostics," (Mirkin, C.A.; 2006).
10. Gordon Research Conference: Nanostructure Fabrication, Tilton, NH; "Unconventional Nanofabrication Technologies," (Mirkin, C.A.; 2006).
11. IEEE-Nano2006, Cincinnati-Ohio, July 17-20, 2006, "Multifunctional Probe Array and Local Vapor Inking Chip for Scanning Probe Nanolithography," (Li, S.; Wang, X.; Liu, C., 2006).
12. 12th Solid State Sensors, Actuator, and Microsystems Workshop (Hilton Head 2006), Hilton Head Island, SC, June 4 - 8, 2006, "A Novel Micromachined Inking Chip for Scanning Probe Nanolithography Using Local Vapor Inking Method," (Li, S.; Shaik, K.A.; Szegedi, S.; Goluch, E.; Liu, E., 2006)
13. BIO2005, Philadelphia, PA; "Big Academia, A Key to Small Science," (Mirkin, C.A.; 2005).
14. Yale Chemical Biology Symposium, Yale University, New Haven, CT; "New Nanotechnological Tools for Studying Biological Systems at the Single Particle Level," (Mirkin, C.A.; 2006).
15. Burgenstock Conference, Burgenstock, Switzerland; "Nanostructures in Chemistry and Biodiagnostics," (Mirkin, C.A.; 2006).
16. Center for Nanoscale Materials Users Meeting: Argonne National Laboratory, Chicago, IL; "Biomolecule Directed Assembly," (Mirkin, C.A.; 2006).
17. PittCon Conference, Orlando, FL; "Massively Parallel Dip-Pen Nanolithography," (2006).
18. PacifiChem 2005 Congress, Honolulu, HA; "On-Wire Lithography (OWL)," (Mirkin, C.A.; 2005).
19. MRS 2005 Fall Meeting, Boston, MA; "Anisotropic Nanostructures: Synthesis, Assembly, and Function," (Mirkin, C.A.; 2005).
20. NanoCommerce/SEMI NanoForum, Chicago, IL; "A Vision for Nanoscience and Nanotechnology," (Mirkin, C.A.; 2005).
21. MIT Materials Seminar Series, Cambridge, MA; "Anisotropic Nanostructures: Synthesis Challenges, Assembly, and Biomedical Applications," (Mirkin, C.A.; 2005).

22. LUX Executive Summit, Cambridge, MA; Panel Member "Nanotech Innovation Outlook: L Leading Scientists Identify Game-Changing Technologies," (Mirkin, C.A.; 2005).
23. 230th ACS National Meeting, Washington, DC; "Bio-Inspired Assembly of Mesoscopic Building Blocks into Functional Architectures," and "Biological Nanoarrays," (Mirkin, C.A.; 2005).
24. UCLA ICCOS XVII Conference, Los Angeles, CA; "The Chemistry and Physical Properties of Self-Organized Nanomaterials" (Mirkin, C.A.; 2005).
25. China International Conference on Nanoscience & Technology (ChinaNANO2005), Beijing, China, June 9-11, 2005, Wang, X., Zou, J., Bullen, D., Dellinger, T., Ryu, K., Liu, C. "MEMS for Nanotechnology Applications - Nanopatterning and Nanomanipulation," (Wang, X.; Zou, J.; Bullen, D.; Dellinger, T.; Ryu, K.; Liu, C.; 2005).
26. Princeton University, Princeton, NJ; "Encoded Nanostructures for Use in Biodiagnostics,"(Mirkin, C.A.; 2005).
27. 228th ACS National Meeting, San Diego, CA; "Nanoarrays for Probing Fundamental Issues in Nanoscience, Chemistry, and Biology," (Mirkin, C.A.; 2005).
28. Nanoscience Seminar Series, Duke University, Durham NC; "Massively Parallel Dip Pen Nanolithography," (Mirkin, C.A.; 2005).
29. MRS 2004 Fall Meeting, Boston, MA; "Massively Parallel Dip Pen Nanolithography," (Mirkin, C.A.; 2004).
30. Beckman Symposium, Irvine, CA; "Tools and Methods that Will Fuel the Nanotechnology Revolution,"(Mirkin, C.A.; 2004).
31. Welch Award Conference, Houston, TX; "Nanostructures in Biodiagnostics: Will They Make a Difference?" (Mirkin, C.A.; 2004).
32. Korean Universities/Physical Society Series, Seoul, Korea; "Dip-Pen Nanolithography: Towards Combinatorial Nanotechnology" and "Encoded Nanostructures for the Detection of Biomolecules," (Mirkin, C.A.; 2004).
33. DARPA Moletronics/MoleApps PI Review, Fairfax, VA; "Nanostructures in Biodiagnostics: Will they make a difference?" (Mirkin, C.A.; 2004).
34. MRS 2004 Spring Meeting, San Francisco, CA; "Combinatorial Nanotechnology Through Massively Parallel DPN," (Mirkin, C.A.; 2004).
35. 11th Solid State Sensor, Actuator, and Microsystems Workshop (Hilton Head 2004), 99-100, Hilton Head Island, SC, 6-10 June 2004, "An Integrated Microfluidic Inking Chip for SPM Nanolithography," (Ryu, K.; Wang, X.; Shaikh, K.A.; Goluch, E.; Bullen, D.; Zou, J.; Liu. C.; 2004).
36. 227th ACS National Meeting, Anaheim, CA; "Building Nanotech Companies in a University Environment," and "DNA-mediated Assembly of Nanostructured Materials: Structure, Properties, and Biodetection Applications," (Mirkin, C.A.; 2004).
37. DARPA Advanced Lithography Program Review, Las Vegas, NV; "Massively Parallel Dip Pen Nanolithography," (Mirkin, C.A.; 2004).
38. AFOSR DPN Workshop, Hawk's Cay, FL; "State of the Art Applications and Future Challenges," (Mirkin, C.A.; 2004).
39. Air Products Seminar, Allentown, PA; "Anisotropic Nanostructures: Synthetic Challenges, Assembly, and Biomedical Applications," (Mirkin, C.A.; 2003).
40. Massachusetts Institute of Technology, Fall 2003 Nanostructures Lecture Series, Boston, MA; "Anisotropic Nanostructures: Synthetic Challenges Assembly and Biomedical Applications," (Mirkin, C.A.; 2003).

41. MRS 2003 Fall Meeting, Boston, MA; "Functional Nanostructures via Dip-Pen Nanolithography," (Mirkin, C.A.; 2003).
42. University of Michigan - Symposium on Frontiers of Nanoscience and Nanotechnology, Ann Arbor, MI; "Nanostructures in Biodiagnostics: Will they make a difference?" (2003).
43. Indiana Biosensor New Ventures Conference, Indianapolis, IN; "Nanostructures in Biodiagnostics: Will they make a difference?" (Mirkin, C.A.; 2003).
44. University of Toronto, Toronto, Canada; "Massively Parallel Dip-Pen Nanolithography: Towards Combinatorial Nanotechnology," (Mirkin, C.A.; 2003).
45. DARPA/DSO Workshop, Pasadena, CA; "DPN and Nanoparticle Probes and their Applications in Signaling and Detection," (Mirkin, C.A.; 2003).
46. Stanford University Student Hosted Colloquium Lecturer, Palo Alto, CA: "Massively Parallel Dip-Pen Nanolithography: Toward Combinatorial Nanotechnology," (Mirkin, C.A.; 2003)
47. DARPA Advanced Lithography Program Review – Santa Fe, NM: "Parallel, Ultrafast Sub-100 Nanometer Dip-Pen Nanolithography," (Mirkin, C.A.; 2003)
49. SmallTalk Conference, San Jose, CA: "Massively Parallel DPN: Towards Combinatorial Chemistry," (Mirkin, C.A.; 2003)

**E. Participating Scientific Personnel**

**Faculty on Project:**

Prof. Chang Liu
Prof. Chad A. Mirkin

**Postdoctoral Associates:**

Tim Dellinger (2005, 50%; 2006)
Shifeng Li (2006)
Joseph Kakkassery (2005, 25%)
Moonhyun Oh (2005, 8%)
Sungho Park (2004, 2005; 2005, 100%)
Nat Rosi (2005, 25%)
Xuefeng Wang (2006)
Jun Zou (2004)

**Graduate Students:**

David Bullen (2004; 2005, 35%)
Lidong Qin (2004; 2005, 50%)
Xuefeng Wang (2005, 100%)

**Other supported personnel**

**2006:** Nandini Topudurti

**F. Invention Disclosures and Patents**

1. "Surface and Site-Specific Ring-Opening Metathesis Polymerization Initiated via Dip-Pen Nanolithography," Mirkin, C.A.; Liu, X.; Guo, S. (NU 23064, Provisional Application 60/488,094).

2. “Self-Organization of Metal-Conducting Polymer Composite Nanowires into 3-Dimensional Tubular Suprastuctures,” Mirkin, C.A.; Park, S.; Lim, J.-H.; Chung, S.-W. (NU 23086, Provisional Application # 60/500,056)
3. “Fabrication of Solid-State Nanostructures Using Resist-Layers Generated by Dip-Pen Nanolithography,” Mirkin, CA.; Zhang, H. (NU 23101)
4. “Scanning Probe Microscopy Probe and Method for Scanning Probe Contact Printing,” Liu, C.; Bullen, D.; Wang, X.; Mirkin, C.A.; Zhang. H. Application filed.
5. “Synthesis of Open-Ended, Cylindrical Au-Ag Alloy Nanostructures on a Si/SiOx Surface,” Mirkin, C.A.; Zhang, H.; Jin, R. (NU 24028)
6. “On-Wire Lithography: High Throughput Nano Gaps and Nano Rod/Disc Arrays,” Mirkin, C.A.; Qin, L.; Park, S.; Huang, L. (NU 25022, Provisional Patent Application 11/372,583)
7. “A Compact Precision XY Micropositions for the Optical Microscope System of Commercial DPN Writes/AFM (Nscriptor) to Locate and Monitor One or Two-D Multiple-probe Array over the Sample Surface” Mirkin, C.A.; Rozhok, S. (NU25041)
8. “Phase Separation Induced Miniaturization of Patterned Structures,” Mirkin, C.A.; Salaita, K. (NU 25062, Provisional Application # 60/697,053)
9. “DPN-Generated Nanostructures as Positive Resists for Preparing Lithographic Masters or Hole Arrays,” Mirkin, C.A.; Salaita, K. (NU 26100)
10. “Universal Method for Direct Patterning Nanobuilding Blocks and Proteins by Dip-Pen Nanolithography,” Mirkin, C.A.; Huang, L.; Kakkassery, J.; Qin, L.; Jang, J.-W. (NU 26112)
11. "Individually addressable, multifunctional probe array for nano through micro scale scanning probe lithography and microscopy,” Liu, C. (US Provisional Patent Application, TF04157).
12. "Scanning Probe Microscope (SPM) Probes with Integrated Capillaries and Fluid Reservoirs," Liu, C. (US Patent Application 10/831,944 and PCT Patent Application US05/13929, TF03038).
13. “Scanning Probe Microscope Probe and Method for Scanning Probe Contact Printing,” Liu, C.; Zou, J.; Wang, X.; Bullen, D. (PCT Patent Application US02/015161)
14. “Electrostatic Nanolithography Probe Actuation Device and Method,” Liu, C. (Patent Application Number 11/377,629)**:**
15. Liu, C.; Zhang, H.; Bullen, D. "Nanoscale Chemical Surface Patterning Dip Pens" (TF01031)

## SCIENTIFIC PROGRESS AND ACCOMPLISHMENTS

### A. Development of New DPN Hardware (Liu)

Scanning probe lithography (SPL) has enabled scientific research down to an unprecedented small scale, and it is capable of nanoscale deposition of an enormous variety of chemical compounds, including organic and biological molecules, polymers, metal salts, and sol-gel precursors. SPL has been widely used for nanoscale patterning and enabled many exciting nanotechnology applications ranging from molecular analysis to nanomaterial synthesis and nanoelectronic fabrication.

The following highlights some of the accomplishments with respect to hardware development that were made by the **Liu** group.

### A.1. Development of New Probes and Probe Arrays

#### A.1.1. 2-D DPN Cantilever Probe Arrays

A major breakthrough was the fabrication of a one million 2-D DPN cantilever probe array using the newly invented mold-and-transfer technique, which was developed for the fabrication of scanning probe microscopy probes with high yield and uniformity. The probes with a tip-to-toe spacing of 50 μm were fabricated on a 5cm$^2$ glass substrate with 100% yield. Two different materials, SU-8 and PDMS were used during the molding process to form pyramidal structures. **Figure 1** shows an example of a PDMS array with a spacing of 5 micron between individual tips. Optimization of the tip-to-tip distance and alignment brought the tip spacing down to hundreds of nanometers. Passive (non-actuated) writing with a prototype 2-D DPN probe array was also demonstrated. A computer controlled 6-degree-of-freedom high-resolution positioning stage was developed for accurately aligning the writing tips with the writing surface, and conductivity-based contact sensors were integrated into the probe array. Finally, a detection circuit was built to sense the contact of probe tip with the writing substrate. By adjusting the contact of the sensing probes at the corners of the probe array, the entire probe array could be accurately aligned with the writing surface. Almost identical patterns were simultaneously generated using this 2-D passive array. In addition, a prototype silicon nitride 7x7 2-D active DPN probe array consisting of 45 writing probes and four integrated contact sensors at the four corners of the array was successfully developed. Each writing probe had a sharp tip and a thermal actuator for lifting the probe tip from the writing surface when actuated. Each sensing probe had an electrode covering its tip and cantilever.

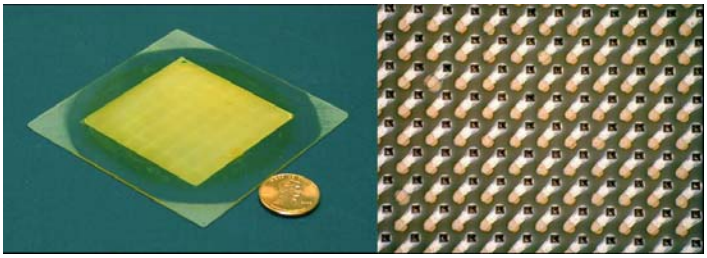

**Figure 1**. A one million 2-D DPN probe array. **Left:** The entire array fabricated on a glass substrate. **Right:** zoom-in micrograph of the high density probes.

#### A.1.2. SPCP Probes and Activated Probe Arrays

In addition to 2-D cantilever probes scanning probe contact printing (SPCP) probes were developed. SPCP uses a scanning probe with an integrated elastomeric (PDMS) tip to directly transfer chemical dot patterns to a substrate. Complex patterns are produced by printing dots in a way similar to dot matrix printing. This new technique combines the chemical versatility and

performance advantage of contact printing with the production flexibility and accuracy of DPN and scanning probe instruments.

Progress was also made in the development of activated probe arrays. New linear 10-DPN probe arrays with electrostatic actuators were developed and tested (**Figure 2**). These probes have electrodes on probe beams and on integrated counter electrode pads. Compared to thermally actuated probes, electrostatic probes have the following design and fabrication advantages: (1) The probe tips are sharper, more uniform, and easier to produce; (2) electrostatic actuation uses less power than thermal actuation, and (3) during operation the entire array is grounded. As a result there is no potential difference between the array and the surface or between adjacent probes in the array. This reduces potential crosstalk effects. Preliminary DPN writing tests using this array have revealed a minimal line width of 30 nm.

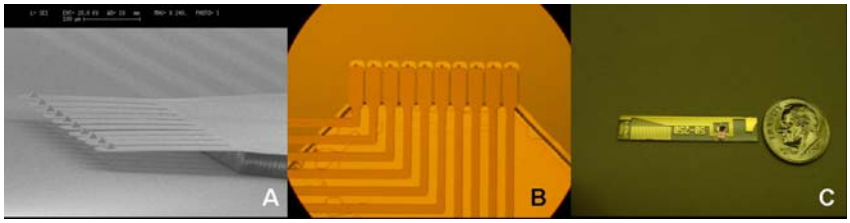


**Figure 2.** The electrostatic DPN probe array. **(A)** An SEM image of the probe array. **(B)** A microscope image of the probe array showing the counter electrode pads, the probes themselves are barely visible past the ends of the electrodes. **(C)** A probe array mounted on a chip holder, ready to be installed on an AFM for DPN writing.

### A.1.3. Development of a Multifunctional Probe Array for Scanning Probe Lithography (SPL) and Microscopy

Traditional Scanning Probe Lithography (SPL) is a serial, single-probe process of low throughput. The main drawbacks limiting its use in industrial applications are small area coverage by individual probes and only one mode of lithography. In addition, complex features consisting of more than one chemical reagent require repeated tip changes and mapping of existing patterns for alignment to prevent cross contamination.

To address these problems, the **Liu** lab developed a multifunctional probe array, consisting of an active probe array for scanning probe lithography in DPN, and scanning probe microscopy in AFM and lateral force microscopy (LFM) modes. This array has the capability of generating as well as imaging patterns covering the nano- through microscale range.

Multifunctional probe arrays composed of tips of different dimensions and tip-to-tip probe distances have two major advantages. They can generate patterns composed of different chemicals as well as image these patterns immediately without risk of cross contamination and the inconvenience of switching probe chips. Furthermore, scanning probe contact printing (SPCP) tips of different sizes will also allow one to generate patterns of different dimensions. SPCP is a DPN variant based on tips made of PDMS rather than silicon nitride.

Individual probes in such an array carry on the cantilevers bimorph thermal actuators, and during lithography they can be lifted independently from the substrate surface. This ensures that only writing or imaging tips are in contact with the surface. Since the tip-to-tip distance is known, accurate registration of patterns generated by different probes in the same array can be achieved.

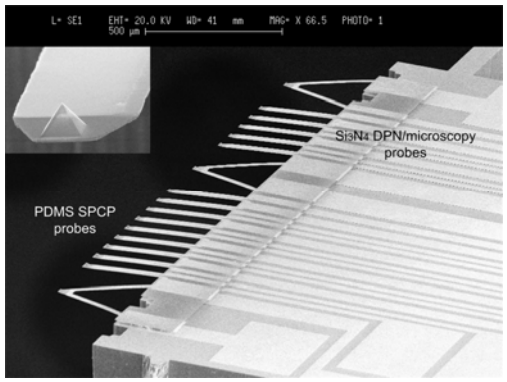


**Figure 3.** SEM image of a multifunctional probe array. Insert: $Si_3N_4$ tip with a 100 nm curvature radius.

A new multifunctional probe array was fabricated using the mold-and-transfer method. Both the probe tips and the cantilevers were fabricated either by molding a $Si_3N_4$ or PDMS elastomer into an etched pit on a Si substrate or through photolithographically patterned $Si_3N_4$. The complete functional probe was then released from the Si substrate by dissolution of the sacrificial layer. **Figure 3** shows a 17-probe chip composed of five rectangular-beam $Si_3N_4$ DPN microscopy tips, three $Si_3N_4$ V-shaped cantilever DPN microscopy tips, and nine $Si_3N_4$ rectangular-beam SPCP probes with PDMS tips. The latter ones come in three different sizes and tip geometries that allow patterning of microstructures of different length scales: round tips with a 300 nm curvature radius suitable for sub-micrometer lithography (3), and flat tops of either 1 μm x 1 μm or 5 μm x 5 μm dimensions (3 of each) for micrometer scale patterning. Furthermore, tips with the same radius of curvature offer redundancy and can be used for different chemicals, while different cantilever shapes provide different force constants and resonant frequencies.

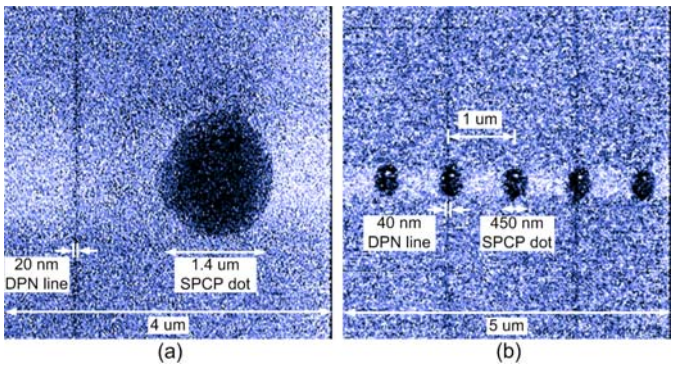


**Figure 4**. LFM images of ODT patterns on a gold surface generated by different probes in the same array. **(a)** 20 nm line pattern and 1.4 μm diameter dot generated by a $Si_3N_4$ DPN tip and a PDMS SPCP tip with a 1 μm x 1 μm flat top, respectively. **(b)** Dots and lines generated by a multifunctional probe array.

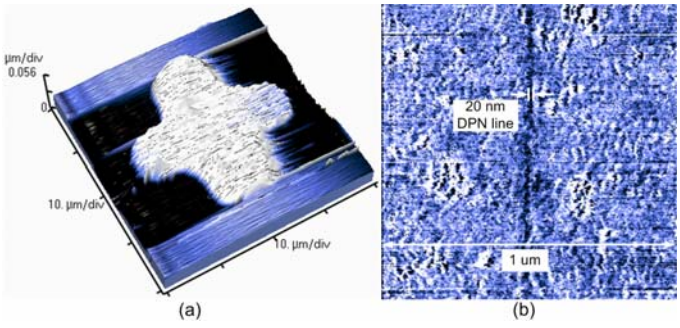


**Figure 5. (a)** 3-D topographic image of a 30 nm dense Au pattern on a Si surface generated in contact mode by a $Si_3N_4$ tip in a multifunctional probe array. Image size is 40 μm x 40 μm. **(b)** LFM image of a 20 nm wide ODT line written by a DPN probe and imaged by a different probe in the same array.

The multifunctional probe array displayed in **Figure 3** was mounted on a Thermomicroscope M5 AFM and tested on a Si surface coated with a 5 nm chrome adhesion layer and a 30 nm gold layer. Octadecanethiol (ODT) was used as ink. $Si_3N_4$ DPN tips can easily create sub-50 nm features, while the blunt PDMS SPCP tips generated patterns in the sub-micrometer and micrometer range. **Figure 4 (a)** displays LFM images of ODT patterns, a 20 nm line and a 1.4 μm dot, both generated using DPN and SPCP probes in the same array. Since the tip-to-tip distance is known, accurate registration between patterns generated by different probes can easily be achieved. **Figure 4 (b)** displays an example of good registration between DPN line and SPCP dot

patterns. The dots were printed first with a PDMS tip, while the line pattern was generated afterwards using a $Si_3N_4$ tip.

The microscopy tips in the multifunctional array allowed us to characterize sample surfaces and to display lithography results in AFM and LFM modes. **Figures 5(a)** and **5(b)** display a topographic image of a 30 nm dense pattern on a Si surface generated by one of the $Si_3N_4$ tips, and an LFM image of a 20 nm wide line generated by DPN and imaged by a microscopy probe in the same probe array, respectively.

### A. 1.4. Pneumatic Actuated PDMS Active Probe for Scanning Probe Nanolithography

Since the existing thermal bimorph actuation method suffers from cross-talking problems that can potentially affect the functions of a scanning probe, new materials and new actuation methods for SPL were explored. The advent of soft lithography has expanded the use of elastomers for surface patterning in many surprising ways. Elastomeric stamps have been used for surface patterning of a variety of different molecules including small molecules such as alkanethiols and silanes and large biomolecules such as DNA and proteins.

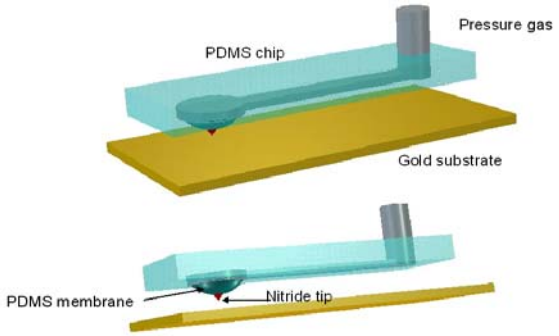


**Figure 6.** Pneumatic actuated PDMS active probe with silicon nitride tip on the membrane.

**Liu** developed a simple PDMS device that takes advantage of the elasticity of PDMS to create a pneumatically actuated surface-patterning tool with unique abilities. The PDMS membrane hosts a pyramidal tip made of PDMS or silicon nitride. A pressured gas line provides inflation pressure to control the contact of the tip with the surface so that ink can be transferred from the tip to the substrate **(Figure 6)**. This device combines the simplicity and versatility of microcontact printing with the resolution of mask-less, scanning probe based lithography methods. Inflation and deflation speed, backing pressure and contact time can be precisely controlled for optimization of the printing process.

For the optimization of the probe design the finite element method was employed. At a contact force and friction force of 10 μN, the PDMS tip showed a size deformation of up to a micron, whereas the silicon nitride tip displayed only minimal deformation. However, at a friction force of 10 μN a silicon tip tilted approximately 600 nm. This suggested that a PDMS device with a PDMS tip required precise positioning facilities in order to reduce the contact force as the large deformation of the PDMS tip made it difficult to generate submicron features on a substrate. Similarly, a PDMS probe with a silicon nitride tip generated only fine features at a smaller friction force.

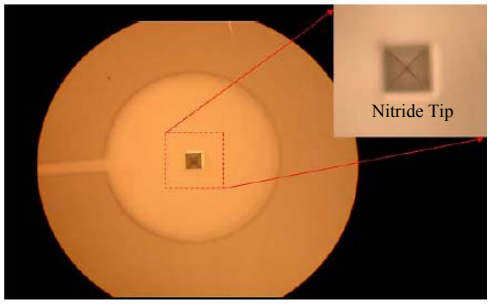


**Figure 7.** Optical picture of a silicon nitride tip on a PDMS membrane.

The PDMS devices were fabricated using the mould and transfer method. The tip mold cavities were etched on the substrate. A 0.3 μm amorphous ZnO layer and a 1μm silicon nitride layer were deposited and patterned on the substrate. The patterned wafer was subsequently treated with $O_2$ plasma, and PDMS prepolymer at a ratio of 20:1 of base to cross-linker coated onto the patterned

silicon wafer. At the same time the PDMS prepolymer was poured into a silicon mold wafer whose surface was treated for 5 minutes with trichloromethylsiloxane, followed by baking at 65°C. Finally the PDMS layer was peeled off the silicon mold wafer and the access holes aligned with the PDMS layer on the patterned silicon wafer. After additional baking at 90°C the bonded device was put into diluted HCL solution for overnight releasing. **Figure 7** displays an optical image of a silicon nitride tip on the PDMS membrane after release.

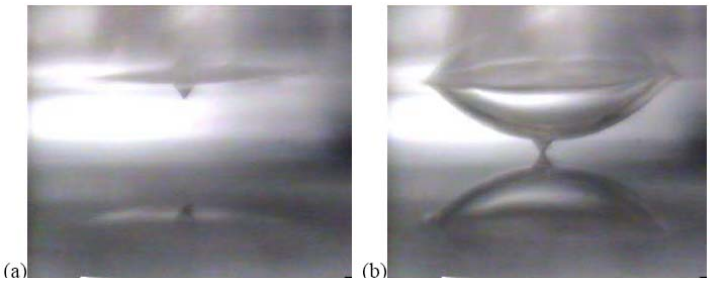


**Figure 8.** Optical micrograph of a PDMS membrane in **(a)** on and **(b)** off states. The refection of the image in **(b)** confirms that the tip really is in contact with the surface.

The PDMS devices were subsequently tested on a Thermomicroscope M5 AFM with ODT as ink, which was transferred to the tip through vapor coating. Briefly, the PDMS devices were attached to the cover of a metal container containing ODT, the container then kept for 30 minutes a 70°C, followed by slow cooling to room temperature. This step was repeated 2 to 3 times until the tips were sufficiently coated with ODT. For patterning the PDMS device was mounted onto the scanning head of a homemade 2-D adaptor and aligned with the optical system inside the scanning head. PDMS is a transparent material that allows one to clearly locate the position of the nitride tip on the patterned substrate. In order to inflate the PDMS membrane pressured gas was delivered to the device through a computer-controlled regulator at a pressure of 5psi. The performance of the tip approaching the substrate was monitored through a CCD camera placed at the front end. Once the tip and surface were in contact, a 2-3 μm over-driving guaranteed that the tip was in contact with the substrate surface. Release of the tip from the surface occurred through reduction of the gas pressure (**Figure 8**).

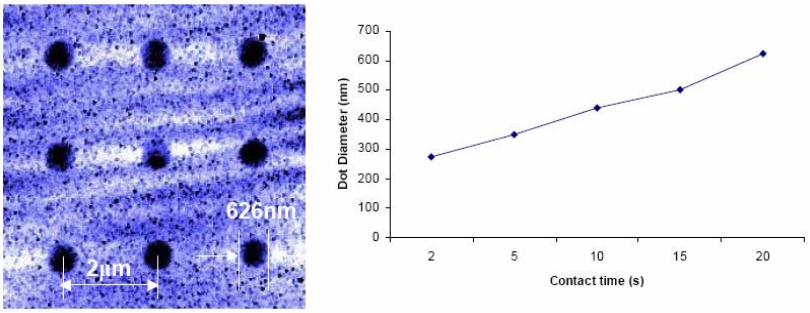


**Figure 9.** ODT dot array fabricated using a pneumatically actuated silicon nitride tip.

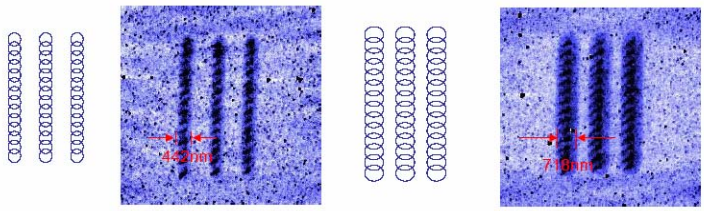

**Figure 10.** Line patterns generated by a dot array matrix.

**Figure 9** shows a six-dot array patterned on a gold-coated substrate generated using a PDMS active probe with a silicon nitride tip at different contact times of 2s, 5s, 10s, 15s and 20s (23°C, 38% relative humidity). **Figure 10** shows line patterns generated by a series of dot

arrays. Contact times of 5s and 10s allowed patterning lines with a width of 442 nm and 718 nm, respectively.

## A.2. Development of New Inking Tools

SPN has been widely used to generate nanometer scale patterns of a variety of materials, including small organic molecules, peptides, proteins, oligonucleotides, and inorganic sol-gels. For subsequent writing onto a substrate the inks must be deposited on the scanning probe tips. This step of probe coating is referred to as inking. Ideally, inking should be fast and efficient, and should allow parallel transfer of ink onto an array of SPN probes. Existing methods of inking include liquid phase inking, inkpad transfer, and vapor phase inking, which all have certain limitations. Liquid phase dip-inking is simple and very popular, but is non-uniform and difficult to control. In addition, this technique suffers from a high rate of ink loss from reservoirs through evaporation as well as cross-contamination when it is used for inking an array. The inkpad-based inking method, which uses a porous membrane (e.g. PDMS) as an ink reservoir has been proposed as an alternative, but the considerable long time of > 6 hours for thiol molecules to diffuse through the thin membrane makes this method rather impractical. Vapor-phase inking on the other hand, which is traditionally done by placing probes into a container of liquid chemical solutions or crystallized chemical compounds, is uniform, reliable, and much faster than liquid phase inking. Unfortunately, this method does not support multi-probe and multi-ink delivery.

### A.2.1. Development of a Microfluidic Inking Chip for Scanning Probe Lithography Inking Tools

An improved microfluidic inking method for the reliable patterning of sub-micron features was developed. This method allowed us to pattern dots ranging in size from 150 nm to 2 μm. With respect to developing multi-channel inking systems, proof-of-concept microfluid inking systems for DPN and SPCP, capable of delivering different inks to probes in a 2-D DPN array, were developed. The design of these systems, which consist of a silicon chip sandwiched by two PDMS pieces (**Figure 11**), was optimized such that ink evaporation during operation could be prevented. Briefly, reservoirs and connecting fluidic channels were formed on the top and bottom PDMS pieces, respectively, and thin PDMS membranes used to cover the opening of the ink channels. Over time the ink diffused from the channel through the membrane to the outer surface, which is in contact with the nanolithography probe tips. This approach was found to minimize the evaporation of liquid ink.

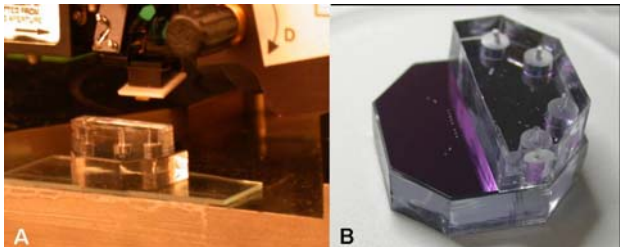


**Figure 11.** The testing setup for inking a DPN/ SPCP probe on an AFM. **(A)** A probe is being brought into contact with the inkpads on the inking chip (**B**) A mirofluid inking chip for DPN and SPCP.

One of the key challenges of current SPL methods is how to increase throughput without impacting pattern size. One way to increase throughput is using one-or two-dimensional probe arrays and coating multiple tips with different inks. Current methods for coating lithography probes with ink require either exposure to chemical vapor or immersion of the probes in an ink solution. However, both of these methods are not applicable to tip arrays due to the potential for cross-contamination and lack of multiple inking capabilities, especially for high-density probe arrays with a tip-to-tip spacing on the order of 100 μm. Parallel inking methods on the other

hand, which use micro-machined open capillary wells, have the disadvantage of losing ink rapidly through evaporation and require monitoring to prevent ink overflow and to maintain the desired liquid level for contact with the SPL tips.

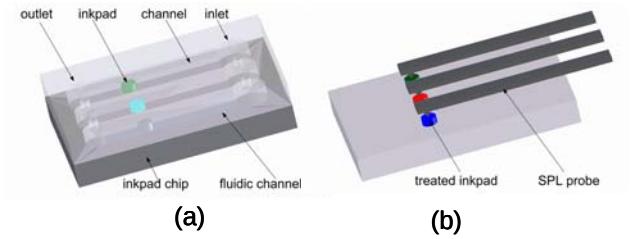


**Figure 12.** Microfluidic contact inking system. **(a)** Microfluidic channel systems for loading each individual inkpad with different inks. **(b)** Contact inking of SPL probes.

A new contact inking system composed of two components, an inkpad chip and a microfluidic channel chip capable of coating lithography probe arrays with different chemical inks was developed (**Figure 12a**). The inkpad chip is fabricated from Si or glass and covered with thin patterned PDMS pad arrays. The channel chip is also composed of PDMS and consists of a set of channels, each with inlet and outlet reservoirs. Individual inkpads are covered by separate microfluidic channels. The physical separation of channels and inkpads on the arrays allows filling simultaneously and in parallel different inks into separate channels as well as multiple individual inkpads. The first step of the inking process is to fill each channel until each inkpad is completely immersed, and ink molecules can diffuse from the channels into the PDMS inkpad. The second step is contact inking of the SPL tips (**Figure 12b)**. After the inkpads were filled with ink, the ink was removed from the channels by a stream of pressurized $N_2$ gas, and the PDMS microfluidic channel chip manually detached from the inkpad chip to expose the treated inkpads. A SPL tip or tip array was then brought into contact with the treated inkpads to initialize ink transfer from the inkpad to the probe tip. After coating with ink, the probe tip is ready for SPL patterning.

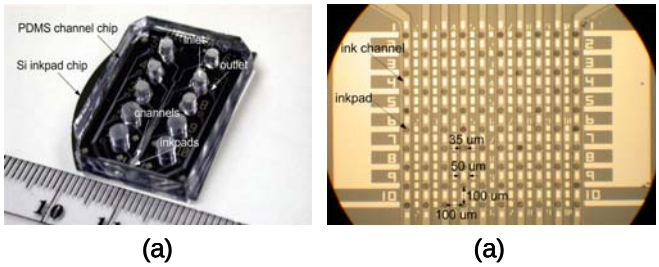


**Figure 13.** Microfluidic inking chip. **(a)** Whole device. **(b)** Microscope image of arrayed inkpads aligned and bonded with the PDMS channels.

**Figure 13** shows a microfluidic inking device consisting of a 10x10 inkpad chip array bonded to a PDMS chip with 10 fluidic channels for simultaneous application of up to 10 different ink solutions. After filling of the ink pads with different ink solutions, they were brought into contact with an SPL probe mounted to an AFM to transfer the ink molecules to the DPN tip. Tip-pad contact was maintained for a set period of time. After removal of the inkpad, the ink-coated SPL tips were ready for writing. **Figure 14** displays LFM images of ODT and MHA patterns generated by commercial $Si_3N_4$ AFM tips coated with ink using our new PDMS inkpads. The ODT and MHA writing tests were done at 26ºC and 42% or 47% relative humidity, respectively. The ODT line widths in **Figure 14a**

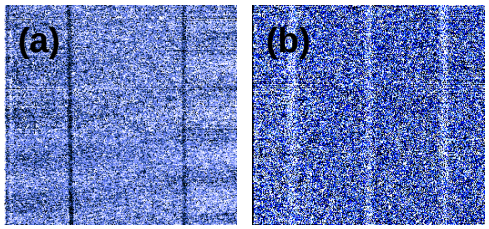


**Figure 14.** LFM images of **(a)** ODT and **(b)** MHA lines generated on a gold surface by an AFM tip in DPN mode. The size of the images is 6 μm x 6 μm.

were 130 nm and 115 nm with writing speeds of 0.1 and 0.2 μm/s for the left and right lines, respectively. The MHA line widths in **Figure 14b** were 200 nm, 175 nm, and 165 nm with writing speeds of 0.4, 0.5, and 0.6 μ/s for the left, middle, and right lines.

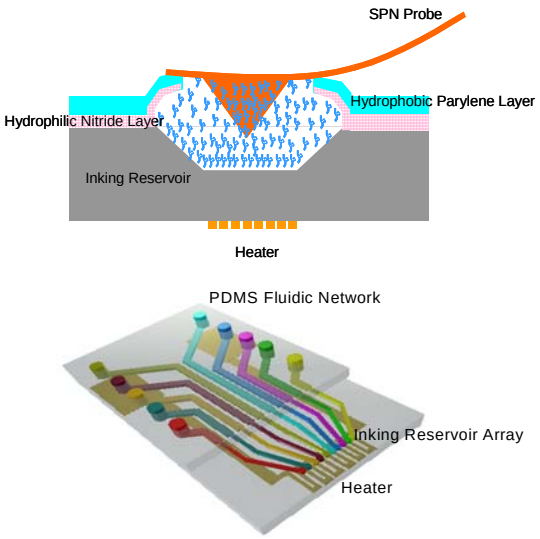


**Figure 15.** Mechanism of local vapor inking for SPL.

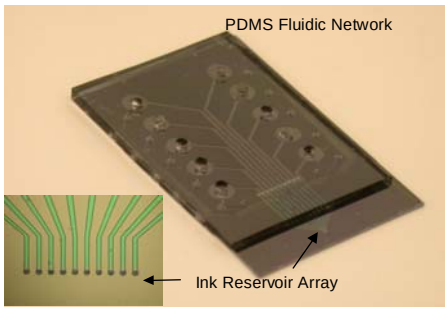


**Figure 16.** Optical picture of an assembled thermal vapor inking chip. The inset is the magnified view of a 10-inking reservoir array.

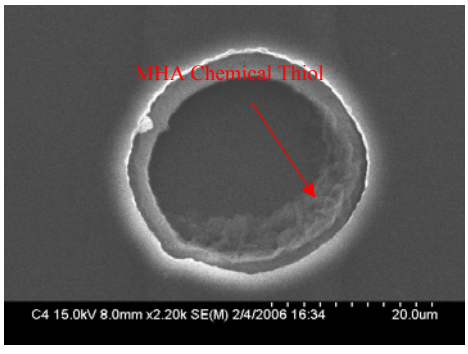


**Figure 17.** Deposition of thiol inside an individual ink reservoir.

### A.2.1. A Micromachined Inking Chip for Scanning Probe Nanolithography (SPN) that Uses Local Vapor Inking

A novel micro-machined chip based on local thermal evaporative inking transfer, for inking of SPN probe arrays was developed. This new inking chip allowed rapid parallel inking in minutes and at a minimal loss of ink. Inks were delivered to closely spaced sites that provide local, on-demand vaporization and ink transfer to the scanning probes.

The structure of an individual inking site is illustrated in **Figure 15**. Each site consists of an ink reservoir with a controlled aperture opening, the size of which matches that of the base on the SPN tips. The reservoirs contained the ink in liquid or crystallized form. An SPN probe was brought to the inking site, and a tight seal formed. The reservoir was locally heated (>60°C), to vaporize the ink molecules and to uniformly coat the SPN probe tip. After cooling of the chip the ink-coated SPN probes could be removed. The inks were supplied to the reservoir through hydrophilic silicon nitride micro channels that automatically pump the thiol solution into individual ink reservoirs due to the dominant surface tension force inside the microchannels. This inking chip was fabricated using micromachining techniques. **Figure 16** is an optical picture of the final assembled inking chip.

In order to validate and characterize the performance of this novel thermal vapor inking chip MHA was used as ink. Briefly, a 1 mM solution of MHA in ethanol was filled into the PDMS channels and automatically pumped into individual ink reservoirs (**Figure 17**). The measured resistance of the thin film heater was around 150 Ω. After application of a 20 DCV bias, the local temperature at the ink reservoirs reached the melting temperature of MHA (64°C) within 2 min. After heating and cooling cycles of 2 minutes each, the inked probe (Type A, NanoInk Inc. Skokie, IL) was loaded onto a scanning probe nanolithography instrument (Nscriptor, Nanoink Inc, Skokie, IL, USA).

**Figure 18** shows MHA patterns on a gold-coated silicon substrate (Au/Cr=30nm/5nm), (top and middle panels). The minimum feature size is less than 60 nm. Using the local thermal vapor inking method, a ten-probe array was inked and used for patterning (**Figure 18, bottom panel**). The line width of the pattern is 130 nm.

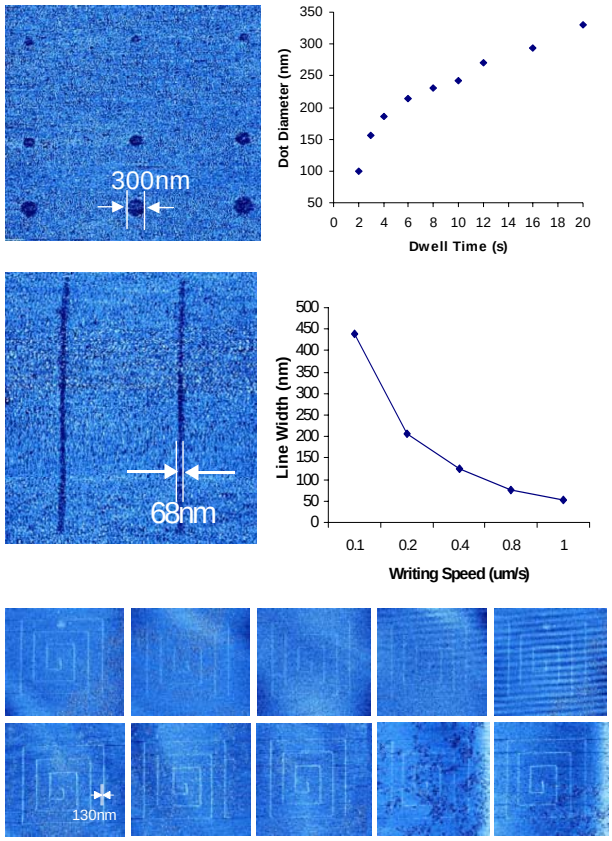


**Figure 18.** (**Top panel**) Characterization of local vapor inking chip dots array writing (3.58 μm by 3.58 μm scanning size), (**middle panel**) lines writing (3.3 μm by 3.3 μm scanning size) at 25 ºC and 30% relative humidity, and (**bottom panel**) the same pattern generated by a ten-pen array simultaneously.

To address the problem of potential cross-contamination during inking, a special ink reservoir that limited cross-contamination was designed. Cross-contamination was limited because each SPN probe was sealed inside an individual reservoir and adjoining ink reservoirs were left empty. Inking of probes using these newly designed reservoirs and their subsequent use for patterning showed that only the inked probes produced patterns. Based on these results one can conclude that local thermal vapor inking limits cross-contamination and allows delivering simultaneously different inks to different ink reservoirs and coating of different probes. The local vapor-inking chip can be reused after two cleaning steps with ethanol/acetone and Piranha to wash away residual ink from the reservoirs and channel, and to render them hydrophilic.

## B. Development of DPN Chemistry and Applications (Mirkin)

### B.1. DNP Applications in Electronics and Biotechnology

#### B.1.1. DNP Applications in Electronics

DPN is a powerful lithographic tool that can be used as a serial deposition tool to synthesize nanosized molecular wires, and deposit diverse, chemically active molecules in very precise orientations and locations. Significant progress was made in developing protocols for the fabrications of electronically active nanostructures (e.g. dots, wires, and gaps) that form the basis for micro- and nanoscale molecular electronic assemblies. In particular, an approach was developed for the fabrication of dot arrays composed

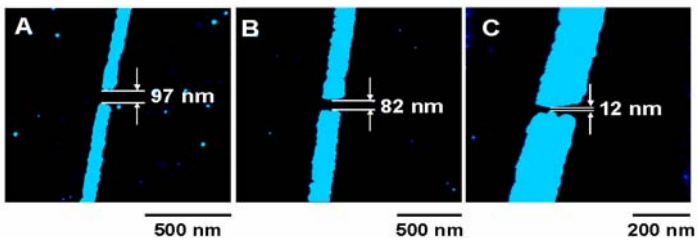


**Figure 19.** TMAFM topographic images of etched Si/$SiO_x$/Ti/Au/MHA nanogaps.

of Au- and Ti-coated silicon oxide with features in the 25-50 nm range. This approach, which was also used to generate nanogaps in the 12-100 nm range, combines high-resolution DPN with wet chemical etching (**Figure 19**). We also developed protocols for the fabrication of arrays with potential electronic applications. Towards this end, high-density nanoscale polymer brush arrays were fabricated using a novel methodology that utilized attributes of DPN and Ring-Opening Metathesis Polymerization (ROMP), and that allowed us to control feature size, shape and inter-feature distance. The capability of delivering monomers using a standard AFM microcantilever and of assembling small monomers with desired active functionalities allowed us to generate small, diverse libraries of nanoscale polymer brushes comprised of large numbers of structurally distinct compounds. **Figure 20** shows a scheme of the procedure for growing polymers from DPN-patterned templates. By using DPN to control the size and shape of the norbornenyl thiol template, and by further controlling the polymerization time (10 minutes to 4 hours), and the choice of the norbornenyl-functionalized monomers, polymer brush nanostructures of different feature sizes covering a range from many micrometers to the sub-100 nm length scale, and different shapes (dots, lines, and other types of geometries) and compositions could be routinely generated. In particular, adjustment of the polymerization time allowed us to control the feature height of the polymer nanostructures over the 1-10 nm range. Using this protocol we could synthesize on gold electrodes arrays of nanoscale polymer brush patterns consisting of electrochemically active monomers, *exo*-5-norbornen-2-yl ferrocenecarboxylate **(1)** and *exo*-5-norbornen-2-yl ferroceneacetate **(2) (Figure 21**). Differential pulse voltammetry (DPV) measurements on the patterns of the polymerized monomer **1** showed an anodic peak at 185 mV vs ($FcH/FcH^+$) (**Figure 21A**) consistent with the solution DPV measurements of the oxidation potential for the norbornenyl ferrocenyl derivative ($E_{pa}$ = 180 mV vs ($FcH/FcH^+$)). In contrast, DPV measurements on the diblock copolymer patterns of the two blocks of electrochemically distinct ferrocenyl monomers **1** and **2** exhibited two anodic peaks at -50 mV and 190 mV that corresponded to the sequential oxidations of the two different types of

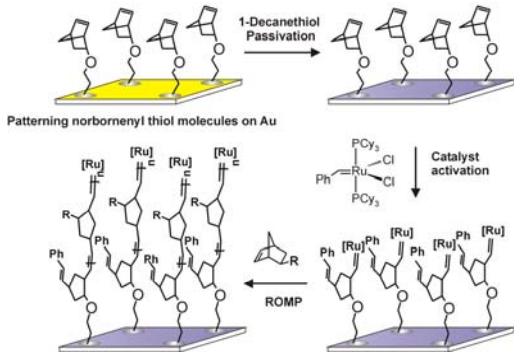


**Figure 20.** A schematic representation of surface-initiated ROMP by DPN.

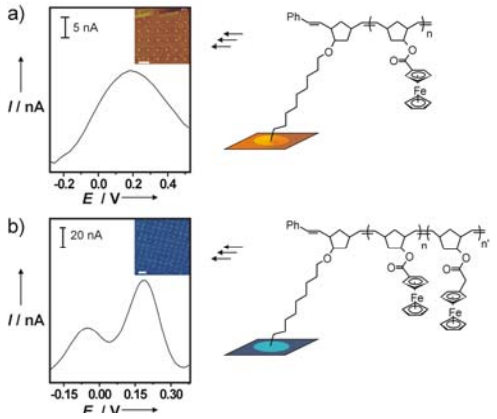


**Figure 21. (A)** DPV of an electrode (0.28 $mm^2$) patterned with poly-1 via DPN and ROMP. **Inset:** AFM topography image of the poly-1 pattern. **(B)** DPV of an electrode patterned with diblock copolymers of monomer 1 and 2 using DPN and ROM. **Inset:** AFM topography image of the diblock copolymer brush pattern. Scan rate: 50 $mVs^{-1}$; pulse period: 200 ms; pulse amplitude: 50 $mVs^{-1}$ and pulse width: 50 ms.

ferrocenyl moieties (**Figure 21B**). These data confirm that indeed the polymers grow from the catalyst-initiated patterns generated by DPN. Using a similar approach consisting of a combination of DPN and ROMP different electronic nanoscale architectures comprised of molecular wires could be fabricated (**Figure 22**). In particular, we successfully synthesized a conductive styrene linker monomer and will use this molecule to construct molecular wires made of polyacetylene. Unlike conventional metals, the electrical properties of conductive polymers such as polyacetylene can be manipulated through the choice of polymer dopant. Transition metals were used for the catalysis of polymerization reactions that created molecular wires that were subsequently connected. Thus far, several photolithography-, electron beam lithography-, and micro-contact printing-based strategies were developed to generate such polymer arrays. However, these methods do not allow us to control nanostructure composition in a site-specific manner, and therefore, do not allow one to fabricate complex multi-component polymer arrays over the nano- to micrometer range.

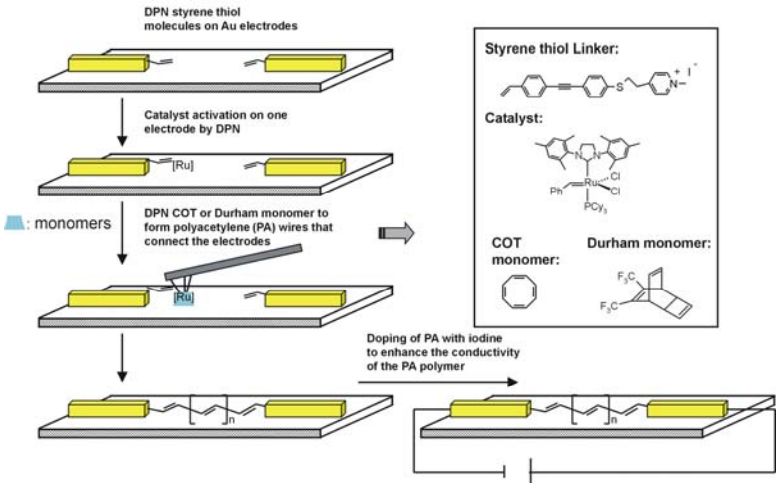


**Figure 22.** Fabrication of Molecular Wires by DPN and Ring-Opening Metathesis Polymerization.

### B.1.2. Using DPN for Bio-Detection Applications

The development of protocols and techniques for the immobilization of biomolecules such as proteins, DNA and viruses in biologically intact form and using these immobilized biomolecular features to trace bioreactions has proven crucial to applications in genomics, proteomics, and diagnostics. With respect to developing DPN as a technology for the fabrication of such soft surface architectures, several important advances were made. It was demonstrated that DPN could be used as a tool to construct nanoarrays with 100 nm feature size, which would allow us to develop nanoassays capable of detecting protein markers for infectious diseases such as AIDS. **Figure 23** displays the DPN-based scheme of the overall fabrication process of such an array composed of negatively charged organic receptor ligands of 16-mercaptohexadecanoic acid (MHA) patterned on a gold thin film. After passivation of unpatterned areas with PEG-alkythiol (11-mercaptoundecyl-tri(ethylene glycol)) mouse monoclonal antibodies to the HIV p24 protein were immobilized on the MHA patterns by immersing the template in a solution containing the anti-p24 antibodies. The applicability of this

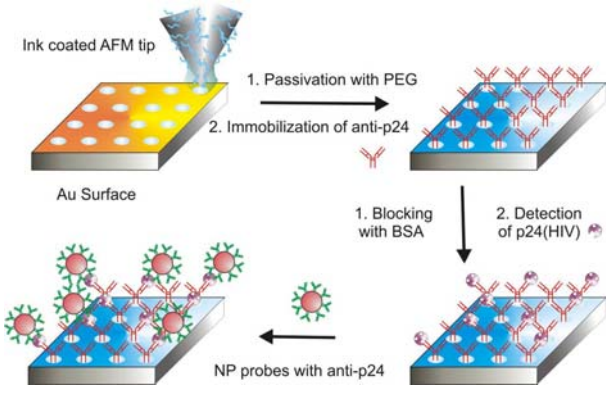


**Figure 23.** Using DPN for the fabrication of an antibody nanoarray.

approach was evaluated by testing the DPN fabricated nanoarray with plasma samples containing the HIV-1 virus. These plasma samples contained 62 and 22 copies/ml of the p24 antigen (**Figure 24**). The result of this experiment represented proof-of-concept for using DPN as a tool to fabricate functional nanoarrays composed of biological structures that can serve as diagnostic tools for biodetection.

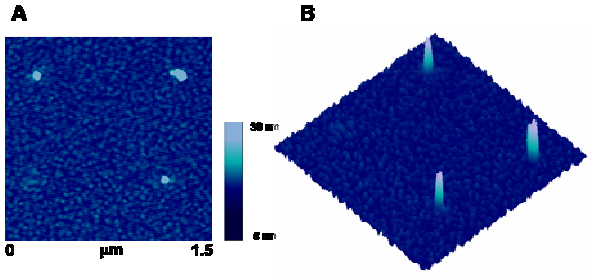


**Figure 24. (A)** Binding of anti-p24 IgG coated Au nanoparticles after p24 protein capture on anti-p24 nanoarrays. **(B)** 3-D image of the nanoarray.

## B.2. Electrochemical Whittling

In order to improve current DPN technology and to develop it into a more accurate and powerful lithography tool electrochemical whittling was developed. This method allowed us to improve the resolution of DPN feature size through post-feature size reduction. Electrochemical whittling is a simple and convenient method for reducing the dimensions of organic micro- and nanostructures on metal surfaces by varying electrochemical desorption conditions. This allowed gradual desorption of DPN features of linear alkanethiols or selenols in a controlled fashion. The whittling process and adsorbate desorption were studied as a function of substrate morphology, adsorbate head and tail groups, electrolyte solvent and salt. Importantly, judicious selection of adsorbate, applied potential, and supporting electrolyte, different nanostructures composed of different adsorbates could be independently addressed and their miniaturization affected (**Figure 25**).

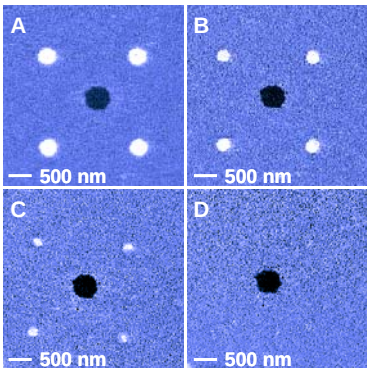


**Figure 25.** LFM images of selective whittling of multi-component nanostructures. **(A)** 2´2 array of MHA (white dots) and ODT (black dots) before application of a potential of -750 mV. The array after application of –750 mV for 3 min **(B)**, 6 min **(C)**, and 9 min **(D)**.

## B. 3. 1-D Parallel Patterning Using Different Tip Configurations

Currently the biggest limitation of DPN is speed, especially in the context of single pen experiments with patterning area limitations that are typically in the range of 100 µm × 100 µm. In order to address this limitation, arrays of cantilevers either in a linear (1-D) or 2-D array format were explored. 1-D parallel patterning with three different tip configurations using a single feedback system in a conventional AFM instrument or the Nscriptor (NanoInk, Inc.), and a simple tip-substrate alignment procedure to ensure that all tips are operational were explored. When such a system was used on a centimeter scale sub-100 nm resolution patterns could be produced. As proof-of-concept experiments sets of lines, dots, crosses, and triangles were patterned on a gold substrate using an MHA-coated A-26 tip array and individual pens (tip speed 0.1 µm/s) (**Figure 26**). The gold substrate was subsequently etched under electrochemical control in a 1 M KOH/1 mM KCN solution, and the resulting MHA protected Au nanostructures imaged using SEM, optical microscopy, and AFM, respectively (**Figure 26 A-C**). Optical micrographs and SEM images, post etching, indicate that all 26 tips were operational (**Figure 26 A, B**). Note the nearly identical line widths, and near flawless nanostructure registration (spacing and orientation between structures). Parallel

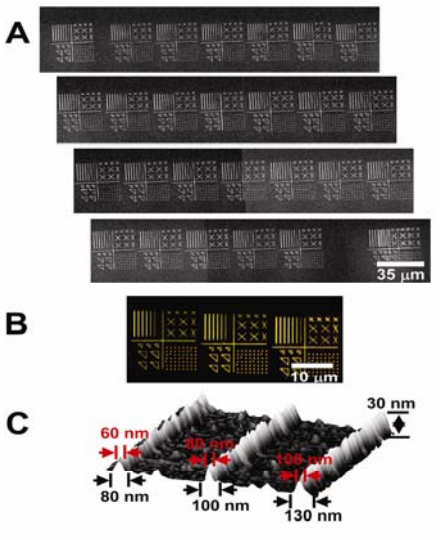


**Figure 26.** (A) SEM images of 26 copies of Au structures (line, triangle, dot and cross) on a Si/SiOx substrate. Actual horizontal image distance is 1 mm, but is divided into four strips and offset vertically for display purposes. (B)

patterning was performed over a distance of 1 mm at a patterning time of less than 15 minutes. Non-contact mode AFM images in **Figure 26 C** indicate that the feature size could be controlled well below 100 nm. With respect to 2-D arrays, the greatest challenge was finding a method to align the plane of the array with that of the substrate, a problem that was solved by using gravity to push the 2-D array into contact and alignment with the substrate, followed by locking the exact position of the tip array using rapidly hardening epoxy.

**Figures 27** and **28** show patterns generated by a 2-D array. The distribution of Au dots matches the spacing of the 2-D array shown in **Figure 27A**. These examples are the first demonstration of patterning covering square centimeter areas by DPN in seconds using a 2D array.

## B.4. DPN to Assemble Multilayer PEM Organic Films

The ability to fabricate features covering the submicron to nanometer range is key to developing novel technological and fundamental applications for DPN. Many structures that are miniaturized in the sub-100 nm size range possess feature-dependent chemical and physical properties. Two important attributes of DPN are its substrate generality and its ability to interface soft organic materials with inorganic substrates. Efforts to expand current applications of DPN patterning have explored a wide range of substrates, from metals to insulators, and a range of different inks including small organic molecules, metal ions, biomaterials, sol gels, nanoparticles, and polymers.

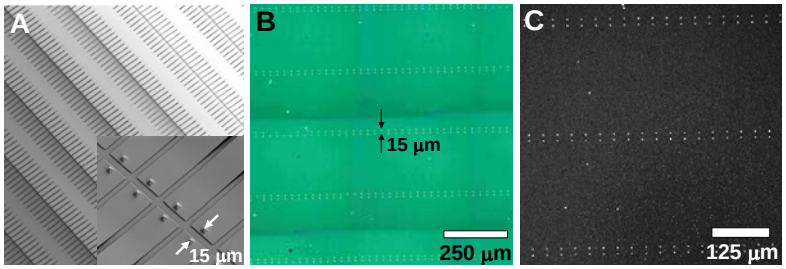


**Figure 27. (A**) SEM images of a 2-D tip array, 1 $cm^2$ contains over 25,000 tips. **(B)** Optical and **(C)** SEM images of a representative area (1 $mm^2$) of 25'000 Au dots patterned using a 2-D pen array.

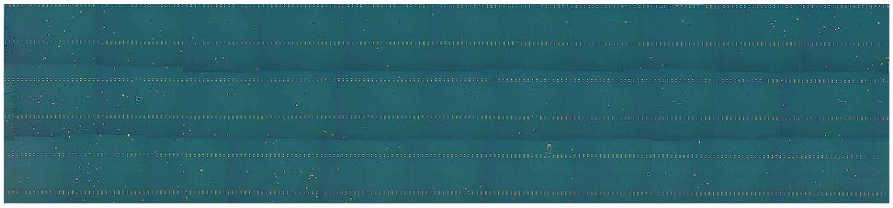

**Figure 28.** Optical micrograph of a representative section of 25,000 Au dots patterned by a 2-D pen array.

Polymers have been extensively used for the fabrication of multilayer films on various substrates using the layer-by-layer (LBL) technique, which allows tailoring and controlling important parameters such as film thickness and the chemical functionality of the film surface. By using an integrated approach that takes advantage of the capabilities of both LBL and DPN techniques, nanometer-size patterns of multilayered polyelectrolyte structures could be

generated. Furthermore, the use of multiple pen arrays allowed us to demonstrate the parallel writing capabilities of DPN in the context of LBL patterning.

Nanometer-size polyelectrolyte multilayer films (PEM) were fabricated using mercaptohexadecanoic acid (MHA) DPN patterns (dots and lines) generated by AFM cantilever probes composed of either 1 or 26 tips. The diameters and widths of the dots and lines varied from 80 to 200 nm, respectively. For passivation a range of molecules including 16-mercapto-1-undecanol (MHO), octadecanethiol (ODT), and 11-mercaptoundecyltri (ethylene glycol) (PEG) were used. PEM films were subsequently prepared by sequentially incubating these substrates in poly(diallyl-dimethylammonium) chloride (PDDA) and poly(sodium-4-styrenesulfonate) (PSS). The substrates were then successively exposed to poly(allylamine) (PAH) and fluorescein sodium salt.

**Figure 29** shows TM-AFM images of PEM organic films adsorbed onto DPN-generated MHA patterns. The diameters of the PEM dot patterns were 200 nm. PEM organic films were generated by electrostatically adsorbing a positively charged polyelectrolyte, PDDA, onto the carboxylic moieties of the MHA template leading to a charge reversal of the PEM surface. This in return enabled the adsorption of the negatively charged PSS polyelectrolyte. Six layers of polyelectrolyte films were generated by sequentially exposing the PEM films to the two different polyelectrolyte solutions.

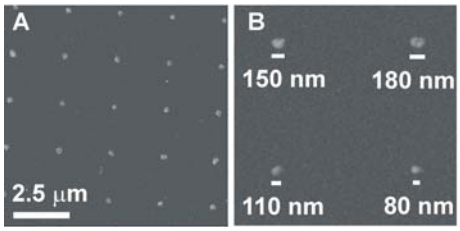


**Figure 29.** Topographical AFM image of (A) 200 nm, (B) 80 to 180 nm dot arrays of PEM ($PE_{PDDA/PSS}$=3)

As a further demonstration of the high-resolution capabilities of the DPN-LBL process, PEM dot patterns with diameters ranging from 80 to 180 nm were fabricated (**Figure 29B**). Since it was previously shown that DPN has the capability to generate MHA features as small as 15 nm, it should be possible to decrease the current PEM dot diameter size of approximately 80 nm further.

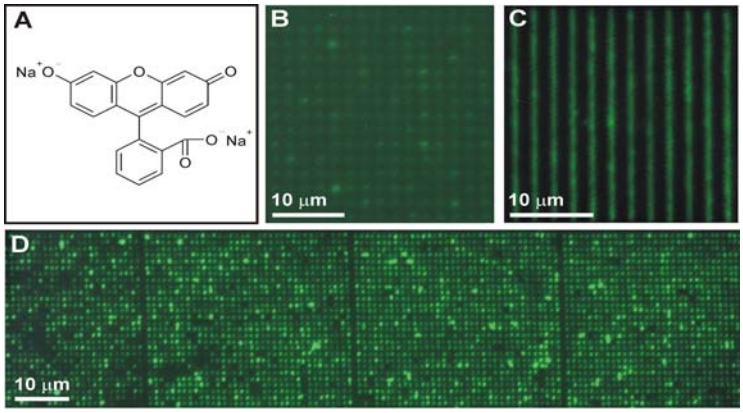


**Figure 30.** Fluorescent images of fluorescein sodium salt. (A) structure, (B, C) adsorbed onto the surface of DPN generated polyelectrolyte multilayer arrays using one, and (D) 26 AFM cantilever tips.

The adsorption of the polyelectrolyte and the build-up of the multilayer films were monitored by TMAFM to measure the height of the dot patterns as a function of the layer number. Adsorption of the polyelectrolytes onto the PEM films led to an increase of the height of the multilayer by 2.3 nm. An increase of the dot sizes of the array from 200 to 500 nm did not increase the height of the patterns after exposure to polyelectrolytes, which suggested that polyelectrolyte adsorption, under the conditions used, was independent of feature size. The potential of DPN-generated PEM organic films for surface immobilization of molecules other than poly-ions was shown by

using PAH and fluorescein sodium salts (**Figure 30**), which could be easily imaged by fluorescence microscopy.

Surface immobilization of PAH and fluorescein was demonstrated by successive immersion of multilayers of polyelectrolytes, electrostatically stacked onto DPN-generated MHA patterns, in a 40 mM PAH or fluorescein sodium salt solution. **Figure 30** shows fluorescent micrographs of PEM organic thin films bearing the fluorescein anion in the top layer of the film. Uniform fluorescein structures on the surfaces of multilayers were observed for DPN-generated PEM organic thin film features of dots and lines (**Figure 30 B, C**).

Multiple near-identical structures could be generated simultaneously when arrays of cantilevers were used. This was demonstrated by using a MHA-coated 26-probe array with a tip-to-tip distance of 35 μm, which generated near identical 200 nm-size dot features (36x72) with an inter-feature center-to-center distance of 900 nm. Ultimately this approach allowed us to generate in 15 minutes 67,000 features. PEMs were subsequently generated on this MHA array template using the LBL approach and labeled with green fluorescein dye (**Figure 30 D**). Despite a defect rate of approximately 4% in the features generated, the overall reproducibility in the mm range is remarkable.

## B.5. DPN as a Tool to Generate Carbon Nanotube Arrays

Single-walled carbon nanotubes (SWNTs) hold great promise as components in a variety of applications ranging from ultra-small devices to multifunctional materials. Currently, a number of SWNT-based proof-of-concept devices such as field effect transistors, field emission displays, and chemical sensors have proven to be smaller, faster, and more sensitive in comparison to existing technologies. The capability to integrate these nanotubes onto surfaces has become a crucial prerequisite for fabrication. Previously different strategies for the positioning of SWNTs onto surfaces were investigated. For example, it was recently shown that SWNTs could be arranged in parallel on the sub-micron scale, by following a molecular approach based on $NH_2$-terminated self-assembled monolayers (SAMs). However, no one thus far was able to control simultaneously the position, shape and linkage of SWNTs on this size scale.

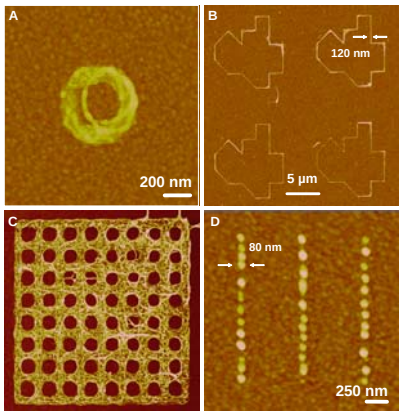


**Figure 31.** TM-AFM topographic images of SWNT arrays. A) SWNT ring. B) Random circuit: the precise positioning, bending and linking of SWNTs following a random MHA pattern is shown. C) SWNT membrane with nanopores of 600 nm diameter. (D) Magnetic carbon- coated iron particles on a MHA pattern.

A simple and reliable DPN-based technique was developed to position, shape and link SWNTs in a variety of structures along the boundary of COOH-SAMs and $CH_3$-SAMs. In a typical experiment, random COOH-terminated features (16-mercaptohexadecanoic acid, MHA) were first patterned by DPN, and the open regions passivated with a $CH_3$- SAM (1-octadecanethiol, ODT). A drop of 1,2-dichlorobenzene containing SWNTs was subsequently rolled through the patterned COOH/$CH_3$ areas. Since 1,2-dichlorobenzene wets COOH-SAMs, but not $CH_3$-SAMs, this movement simply guides SWNTs to the wetting regions containing the COOH patterns. As the tubes were pushed closer, the strong van der Waals attractions of the patterned COOH-SAMs competed with the solvent for the SWNTs. As

a result, individual bundles of SWNTs were trapped on the COOH patterns, and bent to follow precisely the shape of the boundary. This simple methodology not only allowed us to position, but also to shape and connect the SWNTs on the nanometer scale.

For example, SWNT rings of about 500 nm in diameter were first observed as a rare occurrence during nanotube synthesis, but could recently be produced in solution by ultrasonication and ring closure of SWNTs. Using the approach developed by the **Mirkin** lab, SWNT rings could be formed and positioned in an ordered array on a surface. **Figure 31A** displays a TM-AFM image of SWNT rings, formed by connecting 1-4 μm long nanotubes. An array consisting of MHA belts (650 nm in diameter, 170 nm in width) led to the formation of SWNT rings. The shaping of SWNTs into nano letters or the creation of very dense arrays of SWNTs (1 μm × 130 nm lines at a line density of $50M/cm^2$) aligned in parallel could be accomplished in a more controlled fashion. The precise assembly of short SWNTs (10-50 nm) is essential for high performance field effect transistors.

The capability of shaping and interconnecting SWNTs allowed building complicated structures that can potentially be used in a variety of applications. SWNTs could be assembled into arrays of continuous, sub-μm nanowires aligned in parallel (**Figure 31B**). As metallic SWNTs represent an electrical conductivity rival to copper and possess a current carrying capacity of up to $10^9$ $A/cm^2$, which is more than 3 orders of magnitude higher than copper, this new technique may allow SWNTs to be used as conductive interconnects in electronics.

Furthermore, the ability to shape SWNTs allows building in strain through engineering their band gaps. This provides a new tool to organize SWNTs into architectures for different applications. **Figure 31C** displays a "proof-of-concept" SWNT filtration membrane of 9±2 nm thickness for ultra-high filtration flux. The SWNT composition was mapped using a Raman confocal microscope. Since SWNTs are mechanically robust, thermally stable, and electrically conductive, it is reasonable to expect that new applications might emerge for membranes built from SWNTs using this approach.

In conclusion, a new technique was developed that allows one to position, shape, and interconnect μm-long SWNTs along the boundary of COOH-/$CH_3$-SAMs. A variety of DPN guided shapes could be formed without covalent bonding. This technique may be used to direct the assembly of other nano building blocks, such as nanowires and nanoparticles.